The maize aquaporin ZmPIP1;6 enhances stomatal opening and CO_2- and ABA-induced stomatal closure

Lei Ding[1], Maxime J. Laurent[1], Thomas Milhiet [1], Stijn Aesaert[2,3], Mieke Van Lijsbettens[2,3], Laurens Pauwels[2,3,4], Hilde Nelissen[2,3], Dirk Inzé[2,3] and François Chaumont[1]

[1] Louvain Institute of Biomolecular Science and Technology, UCLouvain, 1348 Louvain-la-Neuve, Belgium

[2] Department of Plant Biotechnology and Bioinformatics, Ghent University, 9052 Ghent, Belgium

[3] VIB Center for Plant Systems Biology, Technologiepark 71, 9052 Ghent, Belgium

[4] Current address: Department of Biotechnology, Faculty of Bioscience Engineering, Ghent University, Proeftuinstraat 86, 9000 Ghent, Belgium

Corresponding authors: francois.chaumont@uclouvain.be and lei.ding@uclouvain.be

Total word count: 3999; Introduction: 894; Results: 1626; Discussion: 1479; The number of figures: 8; Figures in color: 7; supplementary figures: 5; supplementary tables: 1.

Running title

PIP1 and stomatal movements

Highlight

Overexpressing the ZmPIP1;6 aquaporin in maize led to increased stomatal opening and accelerated stomatal closure in response to abscisic acid treatment and elevated CO_2 levels compared with wild type plants.

Abstract

The plasma membrane aquaporin *ZmPIP1;6* is expressed in maize stomatal complexes, with higher expression during the day than at night. To elucidate the role of ZmPIP1;6 in gas exchange and stomatal movement, it was expressed in maize (inbred line B104) under the control of *p35S* promoter (OE) or its native promoter fused with *mYFP* cDNA (*mYFP-ZmPIP1;6*). In stomatal complexes of the leaf mature zone, mYFP-ZmPIP1;6 showed higher expression in subsidiary cells than in guard cells, with light and dark treatments influencing its subcellular localization. Notably, ZmPIP1;6 internalization increased in dark conditions versus light. Stomatal opening was greater in *ZmPIP1;6* OE than in wild type (WT), while closure exhibited greater sensitivity to elevated CO_2 concentration or ABA treatment. Our finding revealed that reactive oxygen species (H_2O_2) was involved in ABA-induced stomatal closure, while ZmPIP1;6 was unable to facilitate H_2O_2 diffusion when expressed in yeast. Finally, *ZmPIP1;6* OE and *mYFP-ZmPIP1;6* transgenic plants exhibited higher abaxial stomatal density than WT. Overall, these results indicate that ZmPIP1;6 plays important roles in stomatal opening and CO_2- and ABA-induced stomatal closure.

Keywords

Maize stomata; stomatal movement; aquaporin; CO_2 signaling; ABA signaling; H_2O_2

Introduction

Gas exchanges of CO_2 and water vapor between the plants and the atmosphere take place via stomata, which are micropores in the epidermis of the aerial parts of land plants (Chater *et al*., 2017). Stomata are composed of dumbbell-shaped guard cells (GCs) surrounded by two subsidiary cells (SCs) in grasses like maize, and of two kidney-shaped GCs in other species like Arabidopsis. The opening and closing of stomata depend on variations in the turgor pressure of the GCs and, consequently, on the flow of water and ions across their plasma membrane. In this process, GCs can adjust their volume by ~40% in a few minutes (Franks *et al*., 2001), based on a mechanism of facilitated water diffusion in the membrane.

Aquaporins play important roles in osmotic adjustment during stomatal movement (Ding *et al*., 2024). Aquaporins are small membrane proteins, which facilitate the diffusion of water and other small solutes, and are involved in many physiological processes at different cell, organ, and tissue levels (Chaumont and Tyerman, 2014). Plant aquaporins are grouped into different subfamilies, including plasma membrane intrinsic proteins (PIPs) and tonoplast intrinsic proteins (TIPs). Furthermore, PIPs are phylogenetically divided into two groups, PIP1 and PIP2, that exhibit different subcellular localization and activities when expressed alone in heterologous systems or in maize protoplasts (Chaumont *et al*., 2000; Fetter *et al*., 2004; Zelazny *et al*., 2007). Whereas PIP1s are retained in the endoplasmic reticulum, PIP2s are found in the plasma membrane, but PIP1s and PIP2s can assemble as heterotetramers, resulting in colocalization of both proteins in the plasma membrane and an increase in the cell membrane water permeability (Zelazny *et al*., 2007; Berny *et al*., 2016). Many *PIP* and several *TIP* genes are expressed in stomatal complexes/GCs, such as *AtPIP1;2* and *AtPIP2;1* in *Arabidopsis thaliana* (Kaldenhoff *et al*., 1995; Grondin *et al*., 2015; Ding *et al*., 2024), *HvPIP1;6* in barley (Wei *et al*., 2007), *NtAQP1* in tobacco (Uehlein *et al*., 2008), *SoPIP1;1* in spinach (Fraysse *et al*., 2005), *VfPIP1* in broad bean (Cui *et al*., 2008) and *SunTIP7* and *SunTIP20* in sunflower (Sarda *et al*., 1997). In maize, ZmPIP1;2 and ZmPIP2;1/2;2 were detected in stomatal complexes using immunocytochemistry (Hachez *et al*., 2008). Furthermore, a transcriptomic study of *ZmPIP* gene expression in maize laser-micro-dissected stomatal complexes revealed that almost all *ZmPIP* genes except ZmPIP2;7 were expressed (Heinen *et al*., 2014). Additionally, reverse genetic approaches showed that stomata density, aperture and movement were altered by the deregulation of *PIP* expression in tobacco (Aharon *et al*., 2003; Ding *et al*., 2004), *A. thaliana* (Cui *et al*., 2008; Li *et al*., 2015), *Populus* × *canescens* (Bi *et al*., 2015), soybean (Zhou *et al*., 2014) and rice (Hanba *et al*., 2004) (for review, see Hachez *et al.* (2017)).

Stomatal movement is regulated by various factors including circadian rhythm (Webb, 2003), light (Shimazaki *et al*., 2007), plant water status, pathogens (Melotto *et al*., 2006; McLachlan *et al*., 2014), and several signaling components, such as abscisic acid (ABA) (Pei *et al*., 2000), H_2O_2 (Bright *et al*., 2006; Hua *et al*., 2012) and CO_2 (Zhang *et al*., 2018). Drought stress induces stomatal closure through ABA signaling (Zhu, 2002), a process that regulates aquaporin activity in GCs (Grondin *et al*., 2015; Rodrigues *et al*., 2017; Ding *et al*., 2022). In ABA-induced stomatal closure, ABA binds to RCAR/PYR/PYL receptors, to capture type 2C protein phosphatases, and consequently releasing the inhibition of SnRK2-type protein kinases (SnRK2.6 and OST1) (Raghavendra *et al*., 2010; Wang *et al*., 2016). OST1 protein kinase phosphorylates AtPIP2;1 at Ser-121, enhancing the osmotic water permeability of GCs and stomatal closure (Grondin *et al*., 2015). ABA-induced stomatal closure also results from inward accumulation of H_2O_2 into GCs facilitated by AtPIP2;1 or ZmPIP2;5 (Rodrigues *et al*., 2017; Ding *et al*., 2022). Indeed, H_2O_2 acts as an important secondary messenger in inducing stomatal closure in interaction with ABA and CO_2 signaling pathways (Sussmilch *et al*., 2019). Moreover, when expressed in Xenopus oocytes, AtPIP2;1 facilitates CO_2 diffusion and interacts with carbonic anhydrase, which catalyzes CO_2 to form bicarbonate. Consequently, the accumulation of CO_2 in GCs induces the stomatal closure by activating downstream signaling and membrane transport systems (Chater *et al*., 2015; Zhang *et al*., 2018). However, no difference in high [CO_2]-induced stomatal closure is found in *atpip2;1* mutant and WT plants (Wang *et al*., 2016).

Most *PIPs* are expressed in maize stomatal complexes, with seven of them, Zm*PIP1;1*, Zm*PIP1;2*, Zm*PIP1;3*, Zm*PIP1;5*, Zm*PIP1;6*, Zm*PIP2;1* and Zm*PIP2;2*, accounting for more than 98% of the total *PIPs* transcripts (Heinen *et al*., 2014). Notably, the expression of most *PIP* genes, including ZmPIP1;6, follows a diurnal pattern, with the highest expression during the day. Although ZmPIP1;6 was barely detectable in leaf during the day in the dividing, elongating, or mature zones (Hachez *et al*., 2008), *ZmPIP1;6* appeared to be specifically expressed in stomatal complexes (Heinen *et al*., 2014). Functional analysis revealed that ZmPIP1;6 facilitates transmembrane water diffusion after its co-expression with ZmPIP2;1 isoform in *Xenopus* oocytes, and also facilitates CO_2 diffusion across membranes when expressed alone in yeast. However, direct evidence is still lacking to ascertain whether ABA- and CO_2-induced stomatal movement depends on ZmPIP1s in maize. To address this question, we overexpressed *ZmPIP1;6* in maize B104 genotype and investigated how this overexpression affects stomatal movement. Our results demonstrated that ZmPIP1;6 overexpression enhanced stomatal opening, and stomata closed more rapidly in response to ABA and CO_2 treatments compared with WT plants.

Materials and methods

Transgenic maize plants

To generate *ZmPIP1;6* overexpressing (*ZmPIP1;6* OE) maize lines, *ZmPIP1;6* (Zm00001d020383) was amplified (for the primers, see Table **S1**) and inserted into pBb7m34GW backbone vector (Karimi *et al*., 2013; Ding *et al*., 2020) (https://vectorvault.vib.be/) using User (Hebelstrup *et al*., 2010) and Gateway techniques (Invitrogen, Waltham, MA,US). *ZmPIP1;6* was constitutively overexpressed under the control of *p35S* promoter.

The 3 kb upstream of *ZmPIP1;6* 5`UTR was considered as containing the *ZmPIP1;6* promoter. A 3449 fragment (including 3kb upstream sequence and 5`UTR) was first amplified from B73 gDNA with the forward primer, 5`AGCTTTGGCTTCATCTATGT3` and the reverse primer, 5`CTGCAGCGTGCCTCCTGCCAT3`. This fragment was cloned into pGEM-T Easy vector (Promega) and verified by sequencing. New primers (Table **S1**) were used to amplify a 3,428 bp upstream 5`UTR sequence, and the amplified DNA was cloned into pDONR221 P4-P1r. *mYFP-ZmPIP1;6* was amplified from pCAMBIA-*35S-EYFP-ZmPIP1;6* (Zelazny *et al*., 2007) (for the primers, see Table **S1**). This fragment was inserted into pDONR221 P1-P2. Finally, the *ZmPIP1;6* promoter and *mYFP-ZmPIP1;6* were assembled into the pBb7m24GW expression vector (*ZmPIP1;6::mYFP-ZmPIP1;6)* (https://vectorvault.vib.be/collection/pbb7m24gw).

B104 inbred maize line was transformed according to previous established protocols (Coussens *et al*., 2012; Ding *et al*., 2020; Aesaert *et al*., 2022), at the Crop Genome Engineering Facility of the VIB-UGent Center for Plant Systems Biology, Belgium. The presence of the transgene insertion in the gDNA was checked by PCR (for the primers see Table **S1**). For *ZmPIP1;6* OE maize lines, seven T0 independent lines were obtained and seeds were generated by backcrossing with B104 inbred lines. Two independent lines were selected in this study according to the transgene expression, including one line with relatively low level *ZmPIP1;6* expression (OE-L) and the other with a high level (OE-H). T1 and T2 hemizygous plants segregating for the *ZmPIP1;6* OE and non-transgenic sibling (WT) were used in this study. For *ZmPIP1;6::mYFP-ZmPIP1;6* maize lines, six T0 independent lines were obtained and seeds were generated by backcrossing with B104 inbred lines. Two independent lines were selected in this study, including mYFP-PIP1;6-1 and mYFP-PIP1;6-2. T1 transgenic and non-transgenic sibling plants were used in this study. The plants were grown in phytotron, or greenhouse as described in Ding *et al.* (2020; 2022).

Confocal microscopy

The fluorescence of mYFP in leaves was checked using a LSM 710 confocal microscope equipped with Airyscan module (Carl Zeiss, Oberkochen, Germany). The excitation was 514 nm and emission light was collected with a detector of 520–560 nm.

RNA extraction, real time quantitative PCR (RT-qPCR), protein extraction and western blot

Plants were grown in phytotron with hydroponic culture (Ding *et al*., 2020). Mature zone leaves were collected and flash frozen in liquid N_2 from second leaf of one-week-old maize seedlings. RNA was extracted by using the Spectrum™ Plant Total RNA Kit (Sigma-Aldrich, Mo, US). cDNA synthesis was performed with the M-MLV RT kit (Promega). RT-qPCR was performed with SYBR Green I (Eurogentec, Liège, Belgium) and the signal was detected with StepOnePlus™ Real-Time PCR System (Life Technologies, Foster City, CA, USA). The RT-qPCR program was the same as that described in Ding et al. (2020). $2^{-\Delta Ct}$ method was used to analyze the data, and *EF1α* (Zm00001d046449) and *ACT1* (Zm00001d010159) were used as housekeeping genes. The mean Ct values of the two housekeeping genes was used for normalization using $2^{-\Delta Ct}$ method. Three plants were analyzed for each WT, OE-L and OE-H line, with two technical replicates for each plant. The primers were listed in Table **S1**. To amplify the transgene, the reverse primer was hybridizing the *t35S* terminator.

To prepare plasma membrane fractions, 50 g fresh leaves was ground in a cold room with a blender containing 200 ml extraction buffer (250 mM sorbitol, 50 mM Tris-HCl pH 8.0, 2 mM EDTA) supplemented with 0.6% (w/v) PVP K30, 1 mM phenylmethanesulfonate (PMSF), 0.5 mM dithiotreitol and 2 $\mu g.ml^{-1}$ of protease inhibitors (leupeptin, aprotinin, antipain, pepstatin and chymostatin). A series of centrifugations at 4 °C (770 g for 10 min, 10,000 g for 10 min and 54,000 g for 30 min) was performed to obtain the microsomal fraction pellet. This pellet was resuspended in suspension buffer (330 mM sucrose, 5 mM KH_2PO_4, 3 mM KCl, pH 7.8), and the plasma membrane fraction was isolated by partitioning in an aqueous two-phase system as described by Larsson *et al.* (1987). Western blot analysis was performed according to Hachez *et al.* (2006) and Heinen *et al.* (2014).

Gas exchange

Plants were grown in greenhouse for four weeks and gas exchange measurements were performed with Li-6400XT portable photosynthesis system (LI-COR, Lincoln, Nebraska, USA). The photosynthetic rate (A) and the stomatal conductance (g_s) in response to light intensity were measured at eight light intensities (50, 100, 200, 400, 800, 1200, 1500 and 1800 $\mu mol.m^{-2}.s^{-1}$). During the measurement, CO_2 concentration was maintained at 400 ppm. The light-saturated photosynthetic rate of newly expanded leaves was measured at a light intensity of 1500 $\mu mol.m^{-2}.s^{-1}$. To determine g_s in response to light intensity and CO_2 concentration, the data were automatically recorded by every 20 s. g_s in response to ABA treatment was measured according to Ding *et al.* (2022).

Stomatal density and aperture

Stomatal density was determined by nail polish imprint with newly expanded leaves of four-week-old maize plants grown in the greenhouse. The number of stomata was manually counted from photographs taken using a microscope (DMR, Leica, Germany) equipped with a CCD camera (ORCA-ER C4742-800, Hamamatsu, Japan).

Stomatal aperture was analyzed using two-week-old maize plants grown in a phytotron according to Ding *et al.* (2022). In light-induced stomatal opening measurements, plants were placed in the dark for one hour, leaves were then excised, and stomatal aperture was measured at indicated times. For ABA-induced stomatal closure measurements, 5 μM ABA was applied. Stomatal aperture under different CO_2 treatments was measured according to Hu *et al.* (2010). To obtain stomatal opening buffer containing 400 or 800 ppm CO_2, the buffer was aerated with 400 or 800 ppm CO_2 for 20 min controlled by Li-6400XT. To detect ROS (H_2O_2) during stomatal closure induced by ABA and high CO_2, the peeled epidermis was incubated in the buffer containing 10 μM ABA or different CO_2 concentration. The peels were stained by 10 μM H_2DCFDA according to Ding *et al.* (2022). The aperture size and fluorescence intensity were measured with ImageJ software (http:// rsb.info.nih.gov/ij/).

Leaf temperature

Leaf temperature was measured using a thermal camera (FLIR, USA). Newly expanded leaves were excised from two-week-old maize plants and incubated with 10 μM ABA (diluted with demineralized water) in a glass tube. At the indicated time, the leaves were imaged with thermal camera. The average temperature at 3-6 cm near leaf tip was measured by FLIR Tools (FLIR).

Expression in yeast

Optimized coding sequence of *ZmPIP1;6* (Heinen *et al*., 2014) was amplified and expressed in *Saccharomyces cerevisiae* strain 31019b (*Δmep1–3*) with auxotrophy for uracil and leucine, according to Bienert and Chaumont (2014) and Bienert *et al.* (2018). The fragment was sub-cloned into USER-yeast expression vector pYeDP60u with uracil selection marker and galactose inducible promoter. The constructs containing *ZmPIP2;5* (with leucine selection marker and constitutive promoter), *ZmPIP2;5 H199K* mutant (with leucine selection marker and constitutive promoter) and the empty vectors (either with uracil or leucine selection marker) were obtained from Bienert and Chaumont (2014). Empty vectors and the above-mentioned *PIP* constructs were co-transformed into *Δmep1–3* strain by one-step transformation method (Chen *et al*., 1992). Colonies were selected on synthetic medium (2% (w/v) glucose, 50 mM succinic acid/Tris base (pH = 6.5), 0.7% (w/v) YNB without amino acids, 0.2 % (w/v) amino acids dropout mix without uracil and leucine (Reece-Hoyes and Walhout, 2018), 2% agar). To induce PIP protein expression, 2% galactose was used to replace glucose. For H_2O_2 toxicity assays, different H_2O_2 concentrations were added to synthetic medium (2% (w/v) galactose, 50 mM succinic acid/Tris base (pH = 6.5), 0.7% (w/v) YNB without amino acids, 0.3% (w/v) methionine, 0.3% (w/v) histidine and 2% (w/v) agar), and an OD of 0.01 yeast culture was dropped on the plate. Growth was assessed after 7 days at 30 °C.

Phenotyping

The phenotyping of maize plants was performed at the WIWAM platform (https://www.wiwam.be/phenotyping-systems/wiwam-line/) (Van Hautegem *et al*., 2024, Preprint). The plants were grown in a chamber with a 16-hour light / 8-hour dark cycle at a temperature of 26°C (day) / 21°C (night) and a humidity of 55%, with an approximately light intensity of 170 $\mu mol \cdot m^{-2} \cdot s^{-1}$. This platform was equipped with automated weighing and irrigation capabilities, enabling the implementation of a pre-established irrigation schedule and the imposition of soil water deficit treatments. The well-watered scenario corresponded to no water deficit, with a soil water potential of approximately -0.01 MPa. The water deficit scenario corresponded to a soil water potential of -0.6 MPa. The plants were imaged automatically on a daily basis, and the leaf elongation rate (LER) was determined by measuring the daily length of the fourth leaf from the base of the plant to the tip of the fourth leaf until elongation ceased. The mean LER was calculated

during the entire period of leaf elongation. The final 4th leaf length, width, area as well as the shoot dry weight were measured.

Statistical analysis

Statistical analyses were performed with GraphPad Prism 5 (GraphPad Software). Student's t test was applied to determine the significant differences in Figures 1D, 2, 3G, 5, 7K-L, S1B and S2. Significant differences are indicated by *P < 0.05, **P < 0.01 and ***P < 0.001. ns, not significant. One-way analysis of variance (ANOVA) with Tukey's posttest was applied to compare the significant differences in Figures 3H-I, 4, 6 and 7I-J. Significant differences are indicated by different letters at the level of P < 0.05.

Results

Characterization of transgenic maize lines and expression of *ZmPIP1;6* in stomata

ZmPIP1;6 is expressed in maize stomatal complexes, with higher expression during the day than at night (Heinen et al., 2014). To further elucidate the role of ZmPIP1;6 in gas exchange and stomatal movement, *ZmPIP1;6* was overexpressed (OE) in B104 maize line under the control of *p35S* promoter, active in most plant tissues (Fig. 1A). The mRNA level of the transgene *ZmPIP1;6* in leaves was assessed by RT-qPCR, and two transgenic lines were selected for this study based on their expression levels in the leaf mature zone: one line with relatively low level *ZmPIP1;6* expression (OE-L) and the other with a high level (OE-H) (Fig. 1B). To examine the protein accumulation/abundance difference of ZmPIP1;6 between wild type (WT) and *ZmPIP1;6* OE, plasma membrane proteins were isolated from whole leaves and ZmPIP1;6 was immunodetected using antibodies raised against ZmPIP1;6 (Heinen *et al*., 2014). A more intense signal was observed in both ZmPIP1;6 OE lines than in WT (Fig. 1C,D). The accumulation of ZmPIP1;6 increased approximately 1.6-fold in OE-L and 3-fold in OE-H lines compared with WT plants. No significant difference in signal intensities of PIP2 proteins between WT and ZmPIP1;6 OE plants was observed (Supplementary Fig. S1).

To determine the cell expression pattern of *ZmPIP1;6* in maize leaves, a 3 kb DNA fragment located upstream of *ZmPIP1;6* CDS considered as the promoter, was cloned and used to drive the expression of *mYFP-ZmPIP1;6* (Fig. 1E). In stable transformed maize plants, the

mYFP-ZmPIP1;6 fluorescent signal was detected by confocal microscopy in the leaf elongation zone and mature zone (Fig. 1F). In the elongation zone, the signal in immature stomatal complexes was much weaker compared with the signal in epidermal cells. In the mature zone, the mYFP signal was more intense in SCs than in GCs. The localization of mYFP-ZmPIP1;6 was affected by light conditions, with a more internalized signal notably around the nucleus probably corresponding to the endoplasmic reticulum, observed under dark conditions compared with stomatal complexes exposed to light (Fig. 1F).

Stomatal opening is enhanced by *ZmPIP1;6* overexpression

To determine the role of ZmPIP1;6 in photosynthesis, gas exchange was measured in *ZmPIP1;6* OE and WT plants. Firstly, the photosynthetic rate and the stomatal conductance (g_s) were measured under different light intensity with OE-H and WT plants. A significant increase in both parameters was observed in OE-H compared with WT under a light intensity of 1500 and 1800 $\mu mol.m^{-2}.s^{-1}$, respectively (Supplementary Fig. S2). For the following gas exchange measurements in this study, we used a light intensity of approximately 1500 $\mu mol.m^{-2}.s^{-1}$. g_s increased by 7% in OE-L and 27% in OE-H plants in comparison with WT plants, although the increase in OE-H was not significant. Photosynthetic rate and transpiration were also higher in both *ZmPIP1;6* OE plants than in WT (Fig. 2A-F). However, a significant difference was only observed between OE-L and WT plants, not in OE-H plants.

Stomatal aperture under light induction was compared between *ZmPIP1;6* OE and WT. Stomatal aperture was greater in both *ZmPIP1;6* OE than in WT plants after 30 min of light induction (Fig. 2G, H). The kinetics of g_s closure were also compared between WT and *ZmPIP1;6* OE plants, and similar curves were observed in response to light or dark (Supplementary Fig. S3).

CO_2- and ABA-induced stomatal closure is altered in *ZmPIP1;6* OE lines

The kinetic of stomatal movements induced by different [CO_2] might be affected by the accumulation of ZmPIP1;6, which was shown to facilitate CO_2 diffusion across the plasma membrane when expressed in yeast (Heinen et al., 2014). To test this hypothesis, the continuous recording of g_s was compared between WT, *ZmPIP1;6* OE and *mYFP-ZmPIP1;6* plants under changing [CO_2] (Fig. 3A-F). At 400 ppm [CO_2], g_s of OE-L, OE-H and *mYFP-ZmPIP1;6* was higher than WT plants (Fig. 3A, C, E). Upon switching [CO_2] from 100 ppm to 800 ppm, a faster decrease in g_s was observed in OE-H compared with WT (Fig. 3C). To better visualize the change in g_s, the

relative decrease of g_s was calculated (Fig. 3B, D, F), and to quantify this change in g_s, the time taken for g_s to decrease by half ($T_{1/2}$) was calculated (Fig. 3G). $T_{1/2}$ was significantly lower in OE-H plants than in WTs, while this difference was not significant in OE-L and *mYFP-ZmPIP1;6* plants (Fig. 3G).

To further analyze the response of single stomata to [CO_2], epidermal peels were incubated in buffers with different [CO_2] after the stomata were fully opened by light stimulation. Following a 15 min incubation with 800 ppm [CO_2], the stomatal aperture of both *ZmPIP1;6* OE lines exhibited a significant decrease compared with the 400 ppm [CO_2] treatment (Fig. 3H, I), while no significant difference was observed in WT.

While we previously showed that ZmPIP2;5 played roles in ABA-induced stomatal closure (Ding et al., 2022), no data was available regarding PIP1s. We therefore analyzed the stomatal closure under ABA treatments in *ZmPIP1;6* OE and WT lines (Fig. 4A, OE-L; Fig. 4B, OE-H). After 30 min of 5 μM ABA treatment, stomatal aperture decreased significantly in both *ZmPIP1;6* OE lines, while this reduction was significant in WT plants only after 60 min treatment (Fig. 4).

Detached leaves were incubated with 10 μM ABA, and leaf temperature and g_s were recorded in OE-H and WT plants. Thermal images were taken under ABA treatment for 0 min and 30 min (Fig. 5A). In WT, leaf temperature increased significantly after 10 min of ABA treatment compared with the control treatment (Fig. 5B). Under control condition, leaf temperature was significantly lower in OE-H than WT, while no difference was recorded between WT and the previously characterized *ZmPIP2;5 OE* plants (Ding *et al*., 2020, 2022) (Fig. 5C). Following ABA treatment for 30 min, a significant increase in leaf temperature was observed in both OE-H and *PIP2;5* OE plants when compared with WT plants. Furthermore, a more rapid decrease in g_s was observed in OE-H plants compared with WT under ABA treatment (Fig. 5D, E). Additionally, the decrease in g_s was slightly faster in *mYFP-ZmPIP1;6* than in WT after ABA treatment (Supplementary Fig. S4).

The above-mentioned faster stomatal closure may be beneficial due to the high density of stomata (Faralli et al., 2019). To test this hypothesis, we compared stomatal density in *ZmPIP1;6* OE and WT plants. The abaxial stomatal density significantly increased by 10 % and 7 % in *ZmPIP1;6* OE-L and OE-H, respectively, compared with WT, while no difference in adaxial stomatal density was observed (Fig. 6A). Similar higher abaxial stomatal density was measured in both *mYFP-ZmPIP1;6* expressing lines (Fig. 6B).

H_2O_2 accumulates more rapidly in *ZmPIP1;6* OE stomata upon ABA treatments, while not by high [CO_2] treatments

It was reported that ABA-induced stomatal closure also depends on H_2O_2 entry into GCs via its facilitated diffusion through AtPIP2;1 or ZmPIP2;5 (Rodrigues et al. 2017; Ding et al., 2022). To determine whether the faster stomatal closure in *ZmPIP1;6* OE plants was related to the adjustment of cellular H_2O_2 levels, H_2O_2 levels in GCs were assessed by staining with H_2DCFDA under ABA and CO_2 treatments. Under 10 µM ABA treatment for 5 min, a significant increase in fluorescence signal was measured in OE-H GCs compared with the control treatment (Fig. 7A, B, E, F, J), whereas the signal decreased significantly in WT GCs (Fig. 7I). This decrease in H_2O_2 signal in WT GCs after 5 min of ABA treatment was previously observed in *A. thaliana* and maize (Rodrigues et al., 2017; Ding et al., 2022). After 15 min of ABA treatment, an increase in signal was observed in both OE-H and WT GCs compared with the control treatment (Fig. 7C-D, G-H, I-J).

Following a 2 min treatment with 800 ppm [CO_2], a higher fluorescence signal was observed in WT stomata compared with those treated with 400 ppm [CO_2], whereas a lower signal was observed in OE-H stomata than in WT (Fig. 7K). After 5 min treatment with 800 ppm [CO_2], no significant difference in signal intensity was observed between WT and OE-H compared with the 400 ppm [CO_2] treatment (Fig. 7L).

Furthermore, we investigated whether ZmPIP1;6 facilitated the H_2O_2 diffusion in yeast. We previously demonstrated that PIP1s must be co-expressed with an inactive PIP2 isoform (i.e. ZmPIP2;5H199K) to reach the yeast plasma membrane and assess its H_2O_2 transport capacity (Bienert *et al*., 2014). Accordingly, we co-expressed ZmPIP1;6 with ZmPIP2;5H199K and observed minimal inhibition of yeast growth on plates containing 2 mM H_2O_2, whereas yeast expressing ZmPIP2;5 WT exhibited pronounced growth inhibition (Supplementary Fig. S5). The growth of the yeast strains containing the empty vectors or the empty vector in addition to the vector expressing ZmPIP2;5H199K or ZmPIP1;6 was not impacted by the presence of 2 mM H_2O_2. The results indicate that ZmPIP1;6 is not an active channel for H_2O_2 transport when expressed in yeast.

Plant growth is affected in *ZmPIP1;6* OE plants under water deficit conditions

The opening and closure of stomata are affected in *ZmPIP1;6* OE plants, a phenotype that may influence plant behaviour in response to water deficit. To determine the difference in plant

growth between *ZmPIP1;6* OE and WT plants, we compared the leaf elongation rate (LER) of the 4th leaf, its length, width, area and the shoot dry weight under both control and water-deficit conditions (-0.6 MPa). In WT plants, the LER, final length, width, area and the shoot dry weight decreased significantly under water-deficit conditions in comparison to the control (Fig. 8A-E). Interestingly, this decrease was less pronounced and not statistically significant in both *ZmPIP1;6* OE lines, except for width and area in OE-L plants (Fig. 8 C-D) and length in OE-H plants (Fig. 8B). This data indicates that *ZmPIP1;6* OE could mitigate the reduction in maize plants growth in water deficit conditions by a better regulation of stomata closure.

Discussion

ZmPIP1;6 expression affects gas exchange

In C3 species, PIP aquaporins have been shown to play important roles in regulating photosynthesis, by affecting CO_2 transport conductance, i.e., stomatal and mesophyll conductance (Uehlein *et al*., 2003; Flexas *et al*., 2006; Evans *et al*., 2009; Kaldenhoff, 2012). In contrast, in C4 species such as maize, the photosynthetic rate is less restricted by the CO_2 diffusion resistance, due to the mechanism of CO_2-concentration in bundle sheath cells. In this study, we showed that photosynthetic rate, g_s, stomatal aperture and stomatal density increased in *ZmPIP1;6* OE lines (Figs. 2, 6). The high photosynthetic rate and g_s might result from increased stomatal aperture and density in *ZmPIP1;6* OE plants compared with WT. Indeed, gas exchange was shown to be affected by deregulation of PIP expression in plants, by regulating g_s, stomatal aperture and density (Maurel *et al*., 2016; Ding and Chaumont, 2022; Ding *et al*., 2024). In maize, *ZmPIP2;5* OE plants transpired more than WT plants, which is due to the increase in cell and tissue hydraulic conductivity (Ding *et al*., 2020, 2022). In fact, gas exchange is enhanced by maintaining plant hydraulic conductivity. The water channel activity of ZmPIP1;6 was demonstrated after its co-expression with ZmPIP2;1 in *Xenopus* oocytes and swelling assays (Heinen *et al*., 2014). In *ZmPIP1;6* OE maize plants, the hydraulic conductivity of cells and tissues might increase, further affecting gas exchange and stomatal behavior. In this study, stomatal aperture was greater in *ZmPIP1;6* OE plants than in WT (Fig. 2). We hypothesized that turgor pressure may be higher in *ZmPIP1;6* OE GCs than in WT GCs. GC turgor pressure is regulated by a coupled inflow of ions and water coming from the SC or other neighboring cells (Ding et al., 2024). How *ZmPIP1;6* OE would increase the turgor pressure remains to be elucidated. Several PIPs have been shown to transport ions such as Na^+ (Byrt et al., 2017; Tyerman et al., 2021; Ahmed et al., 2024) and, therefore, this channel activity may contribute to regulate GC turgor

pressure, even though the cation fluxes associated with AQPs are several orders of magnitude lower those required and provided via other transporters (Ding et al., 2022, 2024).

Expression of *mYFP-ZmPIP1;6* under the control of its own promoter (~3 kb fragment) showed that the protein is expressed in the epidermis of leaf elongation and mature zones (Fig. 1). Interestingly, the mYFP-ZmPIP1;6 abundance was very low in developing stomatal complexes but high in mature SCs. In addition, internalization of the protein was observed under dark conditions. This result was in accordance with *ZmPIP1;6* mRNA levels that were shown to be high during the day and low at night (Heinen *et al*., 2014). However, little is known about how SCs regulate stomatal movement, but it was proposed that SCs serve as a source-sink of osmolytes to regulate the turgor pressure of GCs (Nunes *et al*., 2020). Here, the high expression of ZmPIP1;6 in SCs suggests that aquaporin-regulated substrate transport in these specific cells plays pivotal roles in influencing stomatal movements. In Arabidopsis, the potassium channel (KC1) expressed in pavement cells tuned the distribution of K^+ in GCs, further affecting stomatal movements (Nieves-Cordones *et al*., 2022). This result supports the hypothesis that SCs or pavement cells present as a source-sink of osmolytes to regulate the stomatal movements.

Role of ZmPIP1;6 in CO_2- and ABA-induced stomatal closure

CO_2-triggered stomatal movement is a consequence of the regulation in both GCs and mesophyll cells (Zhang *et al*., 2018). In GCs, CO_2 enters the cells by either membrane simple diffusion or facilitated diffusion through PIPs, such as AtPIP2;1 in Arabidopsis (Wang *et al*., 2016). In presence of high CO_2 concentration, AtPIP2;1 interacts with carbonic anhydrase (βCA4), which catalyzes the production of bicarbonate, and further activates downstream signaling cascade to induce stomatal closure. However, the kinetic of stomatal movement was not different in Arabidopsis *pip2;1* mutant than in WT plants, which was thought being due to the redundancy of aquaporin genes in stomata (Wang *et al*., 2016). ZmPIP1;5 and ZmPIP1;6 were also shown to facilitate the transport of CO_2 when they were expressed in yeast (Heinen *et al*., 2014). However, direct evidence is still missing that CO_2-induced stomatal movement was disrupted by the deregulation of PIPs aquaporin in planta. Here, we found that *ZmPIP1;6* OE plants exhibited rapid stomatal closure when increasing CO_2 concentration (Fig. 3). This was not observed in *mYFP-ZmPIP1;6* expression plants driven by *ZmPIP1;6* promoter. In this case, the transgene was mostly expressed in SCs, while in *ZmPIP1;6 OE*, the transgene was expressed under the control of the *35S* promoter that is active in both GCs and SCs (Ding *et al*., 2022). Together, these observations suggest that

the *ZmPIP1;6* expression level and/or location was important to regulate CO_2-triggered stomatal movement.

PIPs also play important roles in regulating ABA-induced stomatal closure. Our previous data demonstrated that ZmPIP2;5 enhanced the sensitivity of stomatal closure to water deficit by regulating leaf and/or stomatal hydraulic and H_2O_2 transport in GCs (Ding *et al*., 2022). Here, a similar phenotype was found in *ZmPIP1;6* OE plants. H_2O_2 accumulated faster in *ZmPIP1;6* OE GCs than in WT, suggesting that ZmPIP1;6 might facilitate the transport of H_2O_2 (Fig. 7). However, ZmPIP1;6 did not seem to be a very efficient H_2O_2 channel when it was expressed in yeast (Supplementary Fig. S5). Aquaporins form homo- or hetero-tetramer on plasma membrane and PIP1s, including ZmPIP1;6, need to physically interact with PIP2s to reach the plasma membrane (Zelazny *et al*., 2007). A faster H_2O_2 accumulation in *ZmPIP1;6* OE stomata could be due to specific membrane enrichment of PIP2s, which are known to be efficient H_2O_2 channel (Bienert *et al*., 2014). In Arabidopsis, ABA activates OST1 kinase that phosphorylates Ser-121 of AtPIP2;1, resulting in the activation of water and H_2O_2 channeling to contribute to stomatal closure (Grondin *et al*., 2015; Rodrigues *et al*., 2017).

CO_2-triggered stomatal closure was reported to be both ABA dependent and independent (Chater *et al*., 2015; Hsu *et al*., 2018). These contrasted results might be explained by difference in the methods of g_s and stomatal aperture measurements using the related genetic mutants. However, in Hsu *et al*. (2018), ABA signaling amplified elevated CO_2-induced stomatal closure. Here, we showed that both CO_2- and ABA-induced stomatal closure was enhanced by *ZmPIP1;6* OE in maize stomata, indicating that common regulation mechanisms might be shared by both inducers of stomatal closure. We checked if H_2O_2 was involved in CO_2-induced stomatal closure and observed that H_2O_2 concentration in *ZmPIP1;6* OE GCs was not increased by 800 ppm CO_2 treatment for 2 min, contrary to what was observed in WT GCs (Fig. 7). This result suggests that high [CO_2]-induced rapid stomatal closure in *ZmPIP1;6* OE plants may be independent on H_2O_2 regulation.

Stomatal density was higher in *ZmPIP1;6* OE and *mYFP-ZmPIP1;6* expressing maize plants than in WT (Fig. 6), and it was proposed that high stomatal density resulted in faster change in g_s (Faralli *et al*., 2019). Therefore, faster CO_2- and ABA-induced stomatal movement might also be explained by higher stomatal density in *ZmPIP1;6* OE plants than in WT. We hypothesized that *ZmPIP1;6* OE maize plants increased their stomatal density to compensate the high dynamic of the stomatal movement that could be detrimental in certain conditions and/or specific developmental stages. In fact, stomatal density development is complex and regulated by multiple

genetic factors (Hepworth *et al*., 2015) and environmental stimuli (Chater *et al*., 2015). Altered leaf hydraulics or carbon fixation by deregulating aquaporin expression can possibly affect stomatal development.

We have previously showed that LER was higher in *ZmPIP2;5* OE maize lines than in WT plants under mild water deficit conditions, whereas this difference was not observed under well-watered conditions (Ding *et al*., 2020). We proposed that the changes in the root and leaf hydraulic conductance observed by deregulating *ZmPIP2;5* at the cellular level resulted in an overall change in whole-plant hydraulic fluxes (and leaf water potential) that affects the LER in stress conditions (Parent et al., 2009; Caldeira et al., 2014; Ding et al., 2020). Here, LER was lower, but not significantly different, in both *ZmPIP1;6* OE lines than in WT under control conditions, whereas this trend was opposite under water deficit conditions (Figure 8A). Under control conditions, the greater stomatal opening in *ZmPIP1;6* OE plants than in WTs may induce a more negative leaf water potential leading to a decrease in LER. With rapid stomatal closure induced by ABA (drought) treatments, *ZmPIP1;6* OE plants may prevent excessive water loss and maintain a higher leaf water potential and LER compared to WT plants, a phenotype similar to what was observed in *ZmPIP2;5* OE, where stomata closed more rapidly than in WT plants under ABA and drought treatments, leading to the maintenance of a high LER under water deficit conditions (Ding *et al*., 2022). Finally, plant growth was therefore improved by this stomatal regulation under water deficit conditions in *ZmPIP1;6* OE plants (Figure 8).

Supplementary data

Table S1. List of primers used for the genetic constructs and RT-qPCR

Fig. S1. PIP2 protein expression in WT and *ZmPIP1;6* OE plants.

Fig. S2. Photosynthetic rate (A) and g_s (B) in response to changing light intensity in WT and OE-H plants.

Fig. S3. Change of g_s in response to light on/off.

Fig. S4. Relative decrease in g_s in WT and mYFP-ZmPIP1;6 plants.

Fig. S5. H_2O_2 toxicity assay in yeast expressing ZmPIP1;6, ZmPIP2;5 and ZmPIP2;5 H199K mutant.

Funding Statement

This work was supported by the Belgian National Fund for Scientific Research (FNRS), the Interuniversity Attraction Poles Programme-Belgian Science Policy (grant IAP7/29), and the "Communauté française de Belgique-Actions de Recherches Concertées" (grants ARC11/16-036 and ARC16/21-075). L.D. was a postdoctoral researcher of the FRS-FNRS.

Author contributions

L.D., T.M., and F.C. designed the experiments. L.D., M.L., T.M., and S.A. performed the experiments. L.P. M.V.L. and D. I. supervised the maize transformation. H.N. was in charge of the drought and growth assays. L.D., M.L., T.M., and F.C. analyzed the data. L.D. and F.C. wrote the manuscript. All the authors contributed to the discussion and revision of the manuscript.

Conflict of interest

No conflict of interest declared.

Data availability

The data that support the findings of this study are available from the corresponding author upon reasonable request.

References

Aesaert S, Impens L, Coussens G, Van Lerberge E, Vanderhaeghen R, Desmet L, Vanhevel Y, Bossuyt S, Wambua AN, Van Lijsebettens M et al. 2022. Optimized transformation and gene editing of the B104 public maize inbred by improved tissue culture and use of morphogenic regulators. *Frontiers in Plant Science* **13**: 883847.

Ahmed J, Ismail A, Ding L, Yool AJ and Chaumont F. 2024. A new method to measure aquaporin‐facilitated membrane diffusion of hydrogen peroxide and cations in plant suspension cells. *Plant, Cell & Environment* 47: 527-539.

Aharon R, Shahak Y, Wininger S, Bendov R, Kapulnik Y, Galili G. 2003. Overexpression of a plasma membrane aquaporin in transgenic tobacco improves plant vigor under favorable growth conditions but not under drought or salt stress. *The Plant Cell* ***15***: 439-447.

Berny MC, Gilis D, Rooman M, Chaumont F. 2016. Single Mutations in the Transmembrane Domains of Maize Plasma Membrane Aquaporins Affect the Activity of Monomers within a Heterotetramer. *Molecular Plant* **9**: 986-1003.

Bi Z, Merl-Pham J, Uehlein N, Zimmer I, Mühlhans S, Aichler M, Walch AK, Kaldenhoff R, Palme K, Schnitzler JP et al. 2015. RNAi-mediated downregulation of poplar plasma membrane intrinsic proteins (PIPs) changes plasma membrane proteome composition and affects leaf physiology. *Journal of proteomics* **128**: 321-332.

Bienert GP, Chaumont F. 2014. Aquaporin-facilitated transmembrane diffusion of hydrogen peroxide. *Biochimica et Biophysica Acta (BBA)-General Subjects* **1840**: 1596-1604.

Bienert GP, Heinen RB, Berny MC, Chaumont F. 2014. Maize plasma membrane aquaporin ZmPIP2;5, but not ZmPIP1;2, facilitates transmembrane diffusion of hydrogen peroxide. *Biochimica et Biophysica Acta (BBA)-Biomembranes* **1838**: 216-222.

Bienert MD, Diehn TA, Richet N, Chaumont F, Bienert GP. 2018. Heterotetramerization of Plant PIP1 and PIP2 Aquaporins Is an Evolutionary Ancient Feature to Guide PIP1 Plasma Membrane Localization and Function. *Frontiers in Plant Science* ***9***: 382.

Bright J, Desikan R, Hancock JT, Weir IS, Neill SJ. 2006. ABA-induced NO generation and stomatal closure in Arabidopsis are dependent on H2O2 synthesis. *The Plant Journal* **45***:* 113-122.

Byrt CS, Zhao M, Kourghi M, Bose J, Henderson SW, Qiu J, Gilliham M, Schultz C, Schwarz M, Ramesh SA and Yool A. 2017. Non‐selective cation channel activity of aquaporin AtPIP2; 1 regulated by Ca^{2+} and pH. *Plant, cell & environment* 40: 802-815.

Caldeira CF, Bosio M, Parent B, Jeanguenin L, Chaumont F and Tardieu F. 2014. A hydraulic model is compatible with rapid changes in leaf elongation under fluctuating evaporative demand and soil water status. *Plant Physiology*, **164***:* 1718-1730.

Chater C, Peng K, Movahedi M, Dunn JA, Walker HJ, Liang YK, McLachlan DH, Casson S, Isner JC, Wilson I et al. 2015. Elevated CO_2-induced responses in stomata require ABA and ABA signaling. *Current Biology* **25**: 2709-2716.

Chater CC, Caine RS, Fleming AJ, Gray JE. 2017. Origins and evolution of stomatal development. *Plant physiology* **174**: 624-638.

Chaumont F, Tyerman SD. 2014. Aquaporins: highly regulated channels controlling plant water relations. *Plant physiology* **164**: 1600-1618.

Chen DC, Yang BC, Kuo TT. 1992. One-step transformation of yeast in stationary phase. *Current genetics* **21**: 83-84.

Chen ZH, Chen G, Dai F, Wang Y, Hills A, Ruan YL, Zhang G, Franks PJ, Nevo E, Blatt MR. 2017. Molecular evolution of grass stomata. *Trends in Plant Science* **22**: 124-139.

Coussens G, Aesaert S, Verelst W, Demeulenaere M, De Buck S, Njuguna E, Inze D, Van Lijsebettens M. 2012. Brachypodium distachyon promoters as efficient building blocks for transgenic research in maize. *Journal of experimental botany* **63**: 4263-4273.

Cui XH, Hao FS, Chen H, Chen J, Wang XC. 2008. Expression of the *Vicia faba* VfPIP1 gene in *Arabidopsis thaliana* plants improves their drought resistance. *Journal of Plant Research* **121**: 207-214.

Ding L, Chaumont F. 2020. Are Aquaporins Expressed in Stomatal Complexes Promising Targets to Enhance Stomatal Dynamics? *Frontiers in plant science* **11***:*458.

Ding L, Milhiet T, Couvreur V, Nelissen H, Meziane A, Parent B, Aesaert S, Van Lijsebettens M, Inzé D, Tardieu F. 2020. Modification of the expression of the aquaporin ZmPIP2; 5 affects water relations and plant growth. *Plant physiology* **182**: 2154-2165.

Ding L, Milhiet T, Parent B, Meziane A, Tardieu F, Chaumont F. 2022. The plasma membrane aquaporin ZmPIP2;5 enhances the sensitivity of stomatal closure to water deficit. *Plant, Cell & Environment* **45**: 1146-1156.

Ding L, Fox AR, Chaumont F. 2024. Multifaceted role and regulation of aquaporins for efficient stomatal movements. *Plant, Cell & Environment.* DOI: 10.1111/pce.14942

Ding X, Iwasaki I, Kitagawa Y. 2004. Overexpression of a lily PIP1 gene in tobacco increased the osmotic water permeability of leaf cells. *Plant, Cell & Environment* **27**: 177-186.

Evans JR, Kaldenhoff R, Genty B, Terashima I. 2009. Resistances along the CO_2 diffusion pathway inside leaves. *Journal of Experimental Botany **60***: 2235-2248

Faralli M, Matthews J, Lawson T. 2019. Exploiting natural variation and genetic manipulation of stomatal conductance for crop improvement. *Current Opinion in Plant Biology* **49**: 1-7.

Flexas J, Ribas-Carbó M, Hanson DT, Bota J, Otto B, Cifre J, McDowell N, Medrano H, Kaldenhoff R. 2006. Tobacco aquaporin NtAQP1 is involved in mesophyll conductance to CO_2 *in vivo*. *The Plant Journal* **48**: 427-439.

Franks PJ, Buckley TN, Shope JC, Mott KA. 2001. Guard cell volume and pressure measured concurrently by confocal microscopy and the cell pressure probe. *Plant physiology* **125**: 1577-1584.

Fraysse LC, Wells B, McCann MC, Kjellbom P. 2005. Specific plasma membrane aquaporins of the PIP1 subfamily are expressed in sieve elements and guard cells. *Biology of the Cell* **97**: 519-534.

Grondin A, Rodrigues O, Verdoucq L, Merlot S, Leonhardt N, Maurel C. 2015. Aquaporins contribute to ABA-triggered stomatal closure through OST1-mediated phosphorylation. *The Plant Cell* **27**: 1945-1954.

Hachez C, Heinen RB, Draye, X, Chaumont F. 2008. The expression pattern of plasma membrane aquaporins in maize leaf highlights their role in hydraulic regulation. *Plant molecular biology* **68**: 337.

Hachez C, Milhiet T, Heinen RB, Chaumont F. 2017. Roles of aquaporins in stomata. In: Chaumont F, Tyerman SD, eds. *Plant aquaporins*. Springer: 167-183.

Hachez C, Moshelion M, Zelazny E, Cavez D, Chaumont F. 2006. Localization and quantification of plasma membrane aquaporin expression in maize primary root: a clue to understanding their role as cellular plumbers. *Plant Molecular Biology* **62**: 305-323.

Hanba YT, Shibasaka M, Hayashi Y, Hayakawa T, Kasamo K, Terashima I, Katsuhara M. 2004. Overexpression of the barley aquaporin HvPIP2; 1 increases internal CO_2 conductance and CO_2 assimilation in the leaves of transgenic rice plants. *Plant and Cell Physiology* **45**: 521-529.

Hebelstrup KH, Christiansen MW, Carciofi M, Tauris B, Brinch-Pedersen H, Holm PB. 2010. UCE: A uracil excision (USER™)-based toolbox for transformation of cereals. *Plant Methods* **6**: 15.

Heinen RB, Bienert GP, Cohen D, Chevalier AS, Uehlein N, Hachez C, Kaldenhoff R, Le Thiec D, Chaumont F. 2014. Expression and characterization of plasma membrane aquaporins in stomatal complexes of *Zea mays*. *Plant Molecular Biology* **86**: 335-350.

Hepworth C, Doheny-Adams T, Hunt L, Cameron DD, Gray JE. 2015. Manipulating stomatal density enhances drought tolerance without deleterious effect on nutrient uptake. *New Phytologist* **208**: 336-341.

Hsu PK, Takahashi Y, Munemasa S, Merilo E, Laanemets K, Waadt R, Pater D, Kollist H, Schroeder JI. 2018. Abscisic acid-independent stomatal CO_2 signal transduction pathway and convergence of CO_2 and ABA signaling downstream of OST1 kinase. *Proceedings of the National Academy of Sciences* **115**: E9971-E9980.

Hu H, Boisson-Dernier A, Israelsson-Nordström M, Böhmer M, Xue S, Ries A, Godoski J, Kuhn JM, Schroeder JI. 2010. Carbonic anhydrases are upstream regulators of CO_2-controlled stomatal movements in guard cells. *Nature cell biology* **12**: 87-93.

Hua D, Wang C, He J, Liao H, Duan Y, Zhu Z, Guo Y, Chen Z, Gong Z. 2012. A plasma membrane receptor kinase, GHR1, mediates abscisic acid-and hydrogen peroxide-regulated stomatal movement in Arabidopsis. *The Plant Cell* **24**: 2546-2561.

Kaldenhoff R. 2012. Mechanisms underlying CO_2 diffusion in leaves. *Current opinion in plant biology* **15**: 276-281.

Kaldenhoff R, Kölling A, Meyers J, Karmann U, Ruppel G, Richter G. 1995. The blue light-responsive AthH2 gene of Arabidopsis thaliana is primarily expressed in expanding as well as in differentiating cells and encodes a putative channel protein of the plasmalemma. *The Plant Journal* **7**: 87-95.

Karimi M, Inzé D, Van Lijsebettens M, Hilson P. 2013. Gateway vectors for transformation of cereals. *Trends in plant science* **18**: 1-4.

Larsson C, Widell S, Kjellbom P. 1987. Preparation of high-purity plasma membranes. *Methods in enzymology* **148**: 558-568.

Li J, Yu G, Sun X, Liu Y, Liu J, Zhang X, Jia C, Pan H. 2015. AcPIP2, a plasma membrane intrinsic protein from halophyte Atriplex canescens, enhances plant growth rate and abiotic stress tolerance when overexpressed in Arabidopsis thaliana. *Plant cell reports* **34**: 1401-1415.

Maurel C, Verdoucq L, Rodrigues O. 2016. Aquaporins and plant transpiration. *Plant, Cell & Environment* **39**: 2580-2587.

McLachlan DH, Kopischke M, Robatzek S. 2014. Gate control: guard cell regulation by microbial stress. *New Phytologist* **203**: 1049-1063.

Melotto M, Underwood W, Koczan J, Nomura K, He SY. 2006. Plant stomata function in innate immunity against bacterial invasion. *Cell* **126**: 969-980.

Nieves-Cordones M, Azeem F, Long Y, Boeglin M, Duby G, Mouline K, Hosy E, Vavasseur A, Chérel I, Simonneau T, Gaymard F. 2022. Non-autonomous stomatal control by pavement cell turgor via the K+ channel subunit AtKC1. *The Plant Cell* **34**: 2019-2037.

Nunes TD, Zhang D, Raissig MT. 2020. Form, development and function of grass stomata. *The Plant Journal* **101**: 780-799.

Parent B, Hachez C, Redondo E, Simonneau T, Chaumont F and Tardieu F. 2009. Drought and abscisic acid effects on aquaporin content translate into changes in hydraulic conductivity and leaf growth rate: a trans-scale approach. *Plant physiology*, **149**: 2000-2012.

Pei ZM, Murata Y, Benning G, Thomine S, Klüsener B, Allen GJ, Grill E, Schroeder JI. 2000. Calcium channels activated by hydrogen peroxide mediate abscisic acid signalling in guard cells. *Nature* **406**: 731.

Raghavendra AS, Gonugunta VK, Christmann A, Grill, E. 2010. ABA perception and signalling. *Trends in plant science* **15**: 395-401.

Reece-Hoyes JS, Walhout AJM. 2018. Generating Yeast One-Hybrid DNA-Bait Strains. *Cold Spring Harbor Protocols, 2018*.

Rodrigues O, Reshetnyak G, Grondin A, Saijo Y, Leonhardt N, Maurel C, Verdoucq L. 2017. Aquaporins facilitate hydrogen peroxide entry into guard cells to mediate ABA-and pathogen-triggered stomatal closure. *Proceedings of the National Academy of Sciences* **114**: 9200-9205.

Sarda X, Tousch D, Ferrare K, Legrand E, Dupuis J, Casse-Delbart F, Lamaze T. 1997. Two TIP-like genes encoding aquaporins are expressed in sunflower guard cells. *The Plant Journal* **12**: 1103-1111.

Shimazaki KI, Doi M, Assmann SM, Kinoshita T. 2007. Light regulation of stomatal movement. *Annual Review of Plant Biology 58*: 219-247.

Sussmilch FC, Schultz J, Hedrich R, Roelfsema MRG. 2019. Acquiring control: the evolution of stomatal signalling pathways. *Trends in plant science* **24**: 342-351.

Tyerman SD, McGaughey SA, Qiu J, Yool AJ, Byrt CS. 2021. Adaptable and multifunctional ion-conducting aquaporins. *Annual Review of Plant Biology* **72**: 703-736.

Uehlein N, Lovisolo C, Siefritz F, Kaldenhoff R. 2003. The tobacco aquaporin NtAQP1 is a membrane CO_2 pore with physiological functions. *Nature* **425**: 734-737.

Uehlein N, Otto B, Hanson DT, Fischer M, McDowell N, Kaldenhoff R. 2008. Function of Nicotiana tabacum aquaporins as chloroplast gas pores challenges the concept of membrane CO_2 permeability. *The Plant Cell* **20**: 648-657.

Van Hautegem T, Takasaki H, Lorenzo CD, Demuynck K, Claeys H, Villers T, Sprenger H, Debray K, Schaumont D, Verbraeken L, Nelissen H. 2024. Division zone activity determines the potential of drought-stressed maize leaves to resume growth after rehydration. Authorea Preprints, doi: 10.22541/au.172456741.10629205/v1. [Preprint].

Wang C, Hu H, Qin X, Zeise B, Xu D, Rappel WJ, Boron WF, Schroeder JI. 2016. Reconstitution of CO_2 regulation of SLAC1 anion channel and function of CO_2-permeable PIP2;1 aquaporin as CARBONIC ANHYDRASE4 interactor. *The Plant Cell* **28**: 568-582.

Webb AA. 2003. The physiology of circadian rhythms in plants. *New Phytologist* **160**: 281-303.

Wei W, Alexandersson E, Golldack D, Miller AJ, Kjellbom PO, Fricke W. 2007. HvPIP1; 6, a barley (Hordeum vulgare L.) plasma membrane water channel particularly expressed in growing compared with non-growing leaf tissues. *Plant and Cell Physiology* **48**: 1132-1147.

Zelazny E, Borst JW, Muylaert M, Batoko H, Hemminga MA, Chaumont F. 2007. FRET imaging in living maize cells reveals that plasma membrane aquaporins interact to regulate their subcellular localization. *Proceedings of the National Academy of Sciences* **104**: 12359-12364.

Zhang J, De-oliveira-Ceciliato P, Takahashi Y, Schulze S, Dubeaux G, Hauser F, Azoulay-Shemer T, Tõldsepp K, Kollist H, Rappel WJ et al. 2018. Insights into the Molecular Mechanisms of CO2-Mediated Regulation of Stomatal Movements. *Current Biology* **28**: R1356-R1363.

Zhou L, Wang C, Liu R, Han Q, Vandeleur RK, Du J, Tyerman S, Shou H. 2014. Constitutive overexpression of soybean plasma membrane intrinsic protein GmPIP1; 6 confers salt tolerance. *BMC Plant Biology* **14**: 181.

Zhu JK. 2002. Salt and drought stress signal transduction in plants. *Annual Review of Plant Biology* **53**: 247-273.

519 **Figure legends**

520 **Fig. 1.** Genetic constructs and expression of ZmPIP1;6 in the transgenic plants. A and E,
521 Schematic representation of the T-DNA used to overexpress *ZmPIP1;6* (A) and express *mYFP-*
522 *ZmPIP1;6* (E) in B104 maize line. RB, right border; *p*35S, CaMV 35S promoter; mYFP, sequence
523 encoding the yellow fluorescent proteins; *tnos*, terminator of the *A. tumefaciens* nopaline synthase
524 gene; t35S, CaMV 35S terminator; *bar*, the gene conferring resistance to bialaphos; LB, left border.
525 B, Relative expression of *ZmPIP1;6* transgene in leaves determined by RT-qPCR. C, ZmPIP1;6
526 protein levels in WT and *ZmPIP1;6* OE lines (OE-L and OE-H). Plasma membrane protein was
527 extracted from whole leaves (leaves were pooled from n > 3 plants growing in a phytotron) and
528 western blots were carried out using antibodies raised against ZmPIP1;6 and H^+-ATPase (PMA,
529 loading control) (Heinen et al., 2014). The upper and lower bands correspond to the dimers and
530 monomers of ZmPIP1;6, respectively. D, Western blot signal quantification. Data are expressed
531 as the mean ± SE. Student's *t* test was applied to compare the significant difference of protein
532 signal between WT and OE plants at the level of *P < 0.05 and ***P < 0.001. F, mYFP-ZmPIP1;6
533 fluorescence in different leaf zones of transgenic T1 maize plants and in stomatal complexes in
534 light and dark, detected by confocal microscopy. GC, guard cell. SC, subsidiary cell. PC, pavement
535 cell.

536

537 **Fig. 2.** Gas exchange parameters in WT and ZmPIP1;6 OE plants. A-F, Photosynthetic rate, g_s
538 and transpiration rate of plants growing in the greenhouse. Data are expressed as the mean ± SE
539 with n ≥ 6 plants. G and H, Stomatal aperture after different times of light induction. Stomatal
540 aperture was analyzed from n > 50 stomata from leaves coming from three plants growing in a
541 phytotron. Student's *t* test was applied to compare the significant difference of photosynthetic rate,
542 g_s and transpiration rate between WT and OE plants at the level of *P < 0.05, **P < 0.01 and ***P
543 < 0.001.

544

545 **Fig. 3.** Kinetic of g_s in response to changing [CO_2] in WT, *ZmPIP1;6* OE (OE-L and OE-H) and
546 *mYFP-ZmPIP1;6* (two lines of *mYFP-ZmPIP1;6-1 and mYFP-ZmPIP1;6-2*) maize lines. A, C and
547 E, Recording of g_s under 400 ppm, 100 ppm and 800 ppm [CO_2]. B, D and F, Relative decrease
548 in g_s when [CO_2] increased from 100 ppm to 800 ppm. G, Half-time ($T_{1/2}$) of g_s decrease induced
549 by increase in [CO_2]. Data are expressed as the mean ± SE from three independent experiments
550 with plants growing in the greenhouse. Student's *t* test was applied to compare the significant
551 difference of stomatal aperture between WT and OE plants at the level of *P < 0.05. H and I,

552 Comparison of stomatal aperture after 15 min incubation with 400 ppm or 800 ppm [CO_2]. Data
553 are expressed as the mean ± SE with n ≥ 110 stomata from three plants growing in a phytotron.
554 One‐way ANOVA with Tukey's posttest was applied to detect the difference significance at the
555 $P < 0.05$ level between genotypes and treatments. Different letters indicate significant differences.

556

557 **Fig. 4.** Stomatal aperture of WT and *ZmPIP1;6* OE plants (A, OE-L; B, OE-H) upon 10 μM ABA
558 treatment. Data are expressed as the mean ± SE, with n≥19 stomata from three plants growing in
559 a phytotron. One‐way ANOVA with Tukey's posttest was applied to detect the difference
560 significance at the $P < 0.05$ level between genotypes and treatments. Different letters indicate
561 significant differences.

562

563 **Fig. 5.** Leaf temperature (A-C) and g_s (D and E) of WT, *ZmPIP1;6* OE and *ZmPIP2;5* OE plants
564 upon ABA treatment. A, Thermal images under ABA treatment for 0 min and 30 min. B, Change
565 in leaf temperature after adding ABA in WT plants. C, Difference in temperature between
566 *ZmPIP1;6* OE, *ZmPIP2;5* OE and WT plants after ABA treatment for 0 min and 30 min. D and E,
567 Change of g_s upon ABA treatment in WT and OE-H plants. Data are expressed as the mean ± SE.
568 Three leaves were measured for each treatment in B and 10-12 leaves were measured for each
569 genotype in C. Six WT and nine OE-H leaves were measured in D and E. Plants were grown in a
570 phytotron. Student's *t* test was applied to compare the significant difference of temperature and g_s
571 between WT and OE plants at the level of *P < 0.05, **P < 0.01 and ***P < 0.001. ns, not significant.

572

573 **Fig. 6.** Stomatal density in adaxial and abaxial sides of WT, *ZmPIP1;6* OE (OE-L and OE-H) and
574 *mYFP-ZmPIP1;6* (two lines of *mYFP-ZmPIP1;6-1 and mYFP-ZmPIP1;6-2*) new fully expanded
575 leaves. A, WT and *ZmPIP1;6* OE plants. B, WT and *mYFP-ZmPIP1;6* plants. Data are expressed
576 as the mean ± SE, n ≥ 5 plants growing in the greenhouse. One‐way ANOVA with Tukey's
577 posttest was applied to detect the difference significance at the $P < 0.05$ level. Different letters
578 indicate significant differences.

579

580 **Fig. 7.** Reactive oxygen species in stomata under ABA treatment (A-J) and under 400 ppm and
581 800 ppm CO_2 treatment after 2 min (K) and 5 min (L). A-H, the fluorescence signal of ROS in
582 WT and OE-H stomata after ABA treatment for 5 min and 15 min. I and J, the comparison of

583 fluorescence intensity in GCs. Data are expressed as the mean ± SE with n ≥ 20 stomata from
584 three plants growing in a phytotron and individual data was shown in H and I. One‐way ANOVA
585 with Tukey's posttest was applied to detect the difference significance at the $P < 0.05$ level
586 between treatments and time. Different letters indicate significant differences.

587

588 **Fig. 8.** Leaf elongation rate (A) of the 4th leaf, its final length (B), width (C), area (D) and shoot
589 dry weight (E) under control and water-deficit treatments in *ZmPIP1;6* OE (OE-L and OE-H) and
590 their respective WT plants. The values indicate means ± SE (n = 3~9 plants). One‐way ANOVA
591 with Tukey's posttest was applied to detect the difference significance at the $P < 0.05$ level.
592 Different letters indicate significant differences.

593

Figure 1

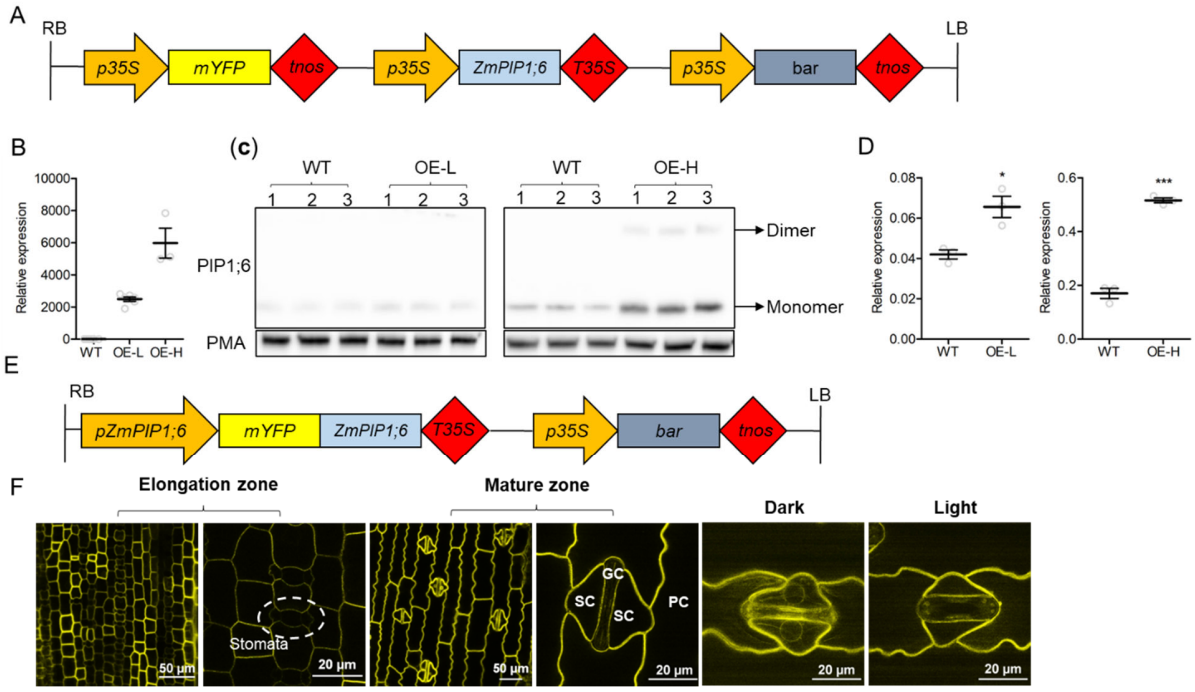
A
RB
p35S
mYFP
tnos
p35S
ZmPIP1;6
T35S
p35S
bar
tnos
LB
B
Relative expression
WT
OE-L
OE-H
(c)
WT
OE-L
WT
OE-H
PIP1;6
PMA
Dimer
Monomer
D
Relative expression
WT
OE-L
WT
OE-H
E
RB
pZmPIP1;6
mYFP
ZmPIP1;6
T35S
p35S
bar
tnos
LB
F
Elongation zone
Mature zone
Dark
Light
Stomata
GC
SC
SC
PC
50 μm
20 μm
50 μm
20 μm
20 μm
20 μm

597 Figure 2

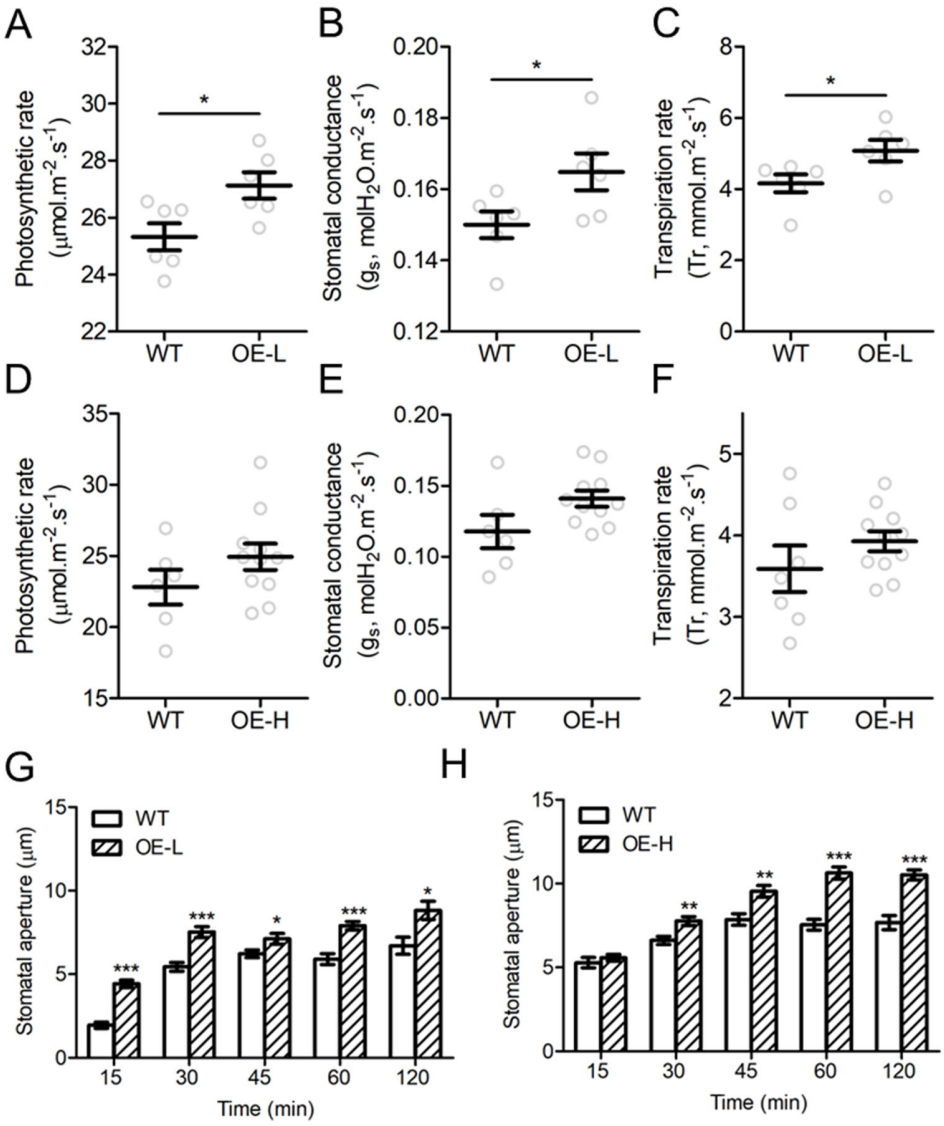

598

599

Figure 3

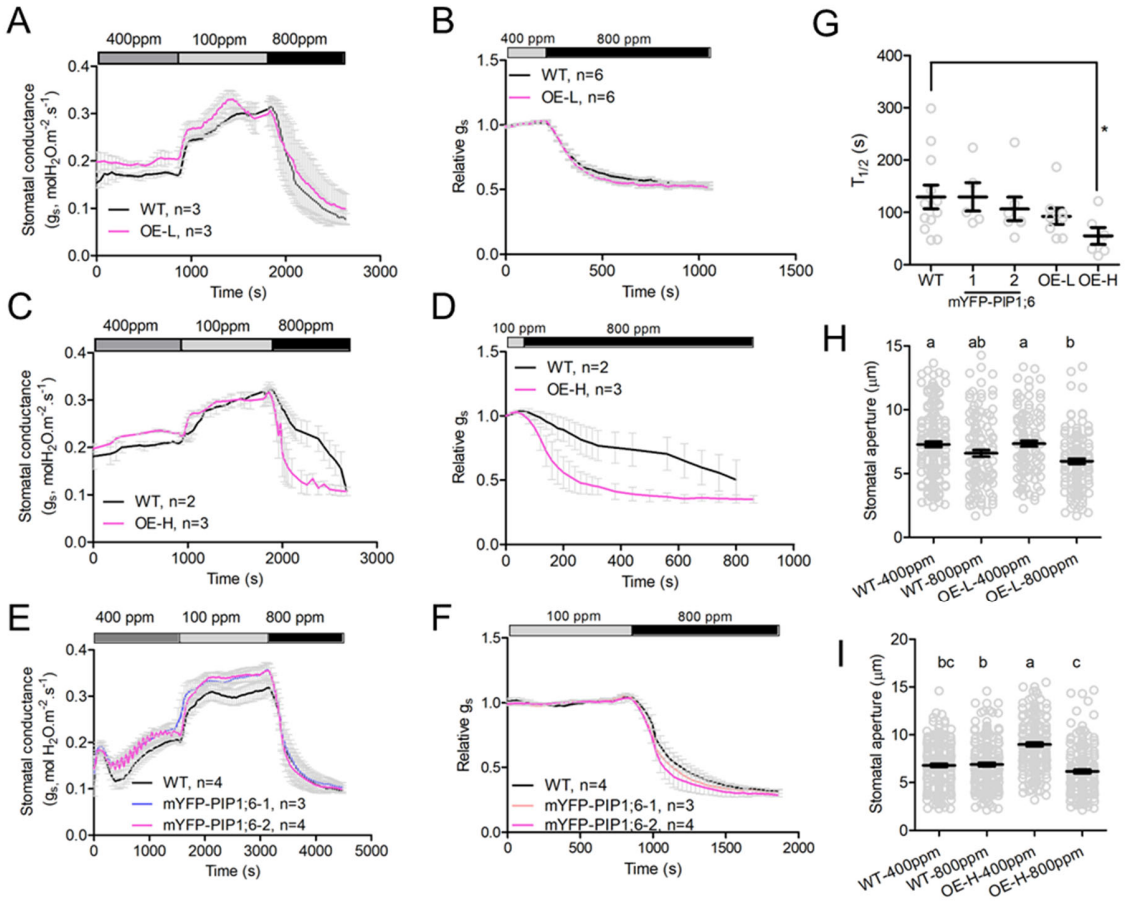
A
400ppm
100ppm
800ppm
Stomatal conductance (gs, molH2O.m-2.s-1)
WT, n=3
OE-L, n=3
Time (s)
B
400 ppm
800 ppm
Relative gs
WT, n=6
OE-L, n=6
Time (s)
G
T1/2 (s)
WT
1
2
OE-L
OE-H
mYFP-PIP1;6
C
400ppm
100ppm
800ppm
Stomatal conductance (gs, molH2O.m-2.s-1)
WT, n=2
OE-H, n=3
Time (s)
D
100 ppm
800 ppm
Relative gs
WT, n=2
OE-H, n=3
Time (s)
H
Stomatal aperture (μm)
a
ab
a
b
WT-400ppm
WT-800ppm
OE-L-400ppm
OE-L-800ppm
E
400 ppm
100 ppm
800 ppm
Stomatal conductance (gs, mol H2O.m-2.s-1)
WT, n=4
mYFP-PIP1;6-1, n=3
mYFP-PIP1;6-2, n=4
Time (s)
F
100 ppm
800 ppm
Relative gs
WT, n=4
mYFP-PIP1;6-1, n=3
mYFP-PIP1;6-2, n=4
Time (s)
I
Stomatal aperture (μm)
bc
b
a
c
WT-400ppm
WT-800ppm
OE-H-400ppm
OE-H-800ppm

603 Figure 4

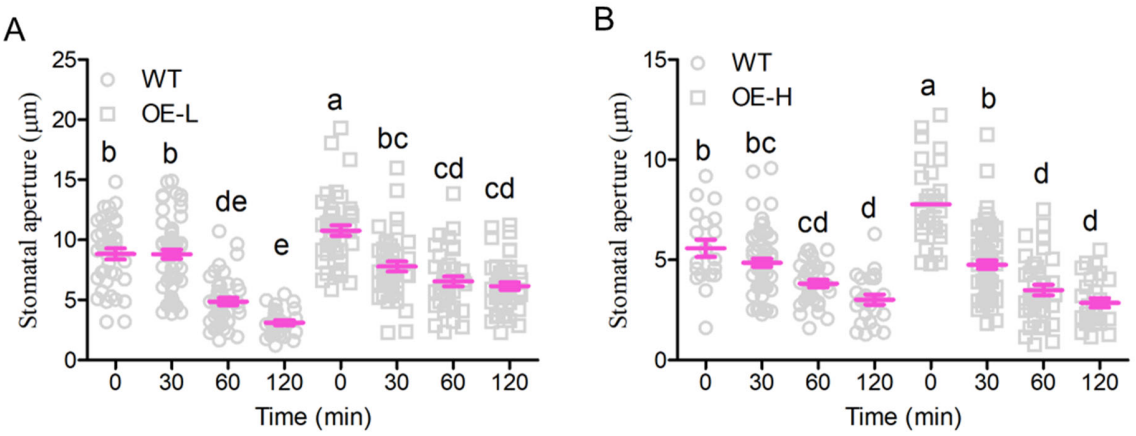

604

605

606 Figure 5

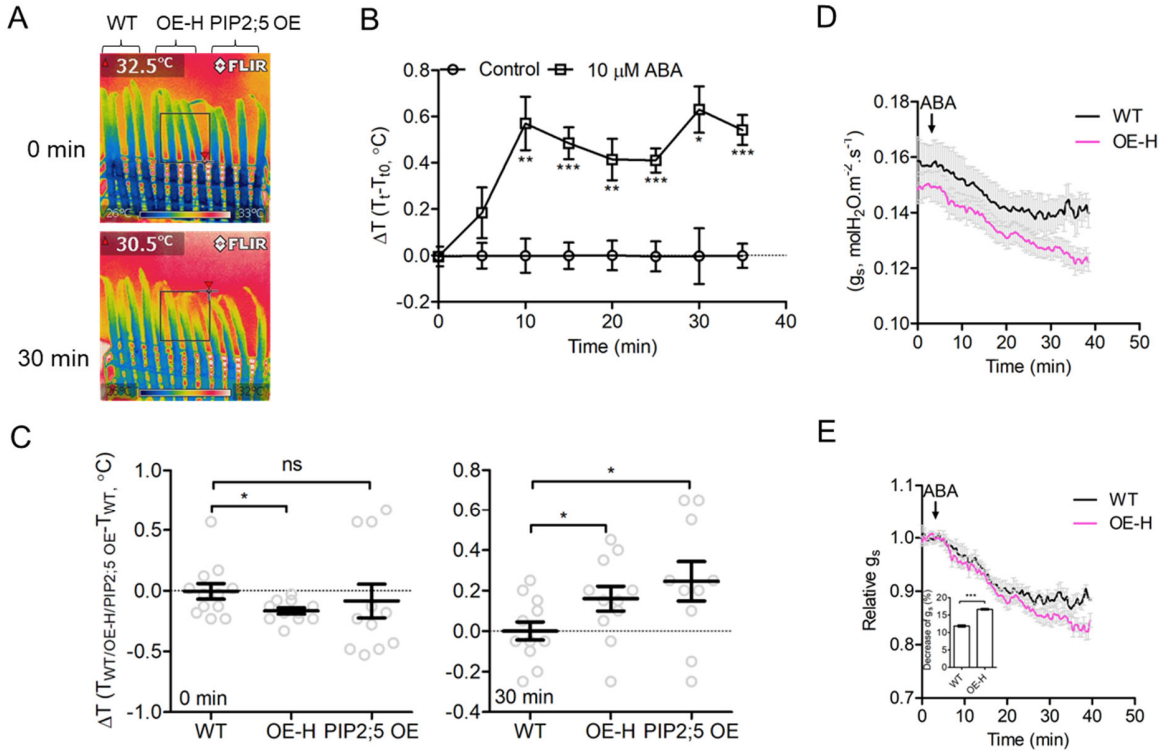

607

608

609 Figure 6

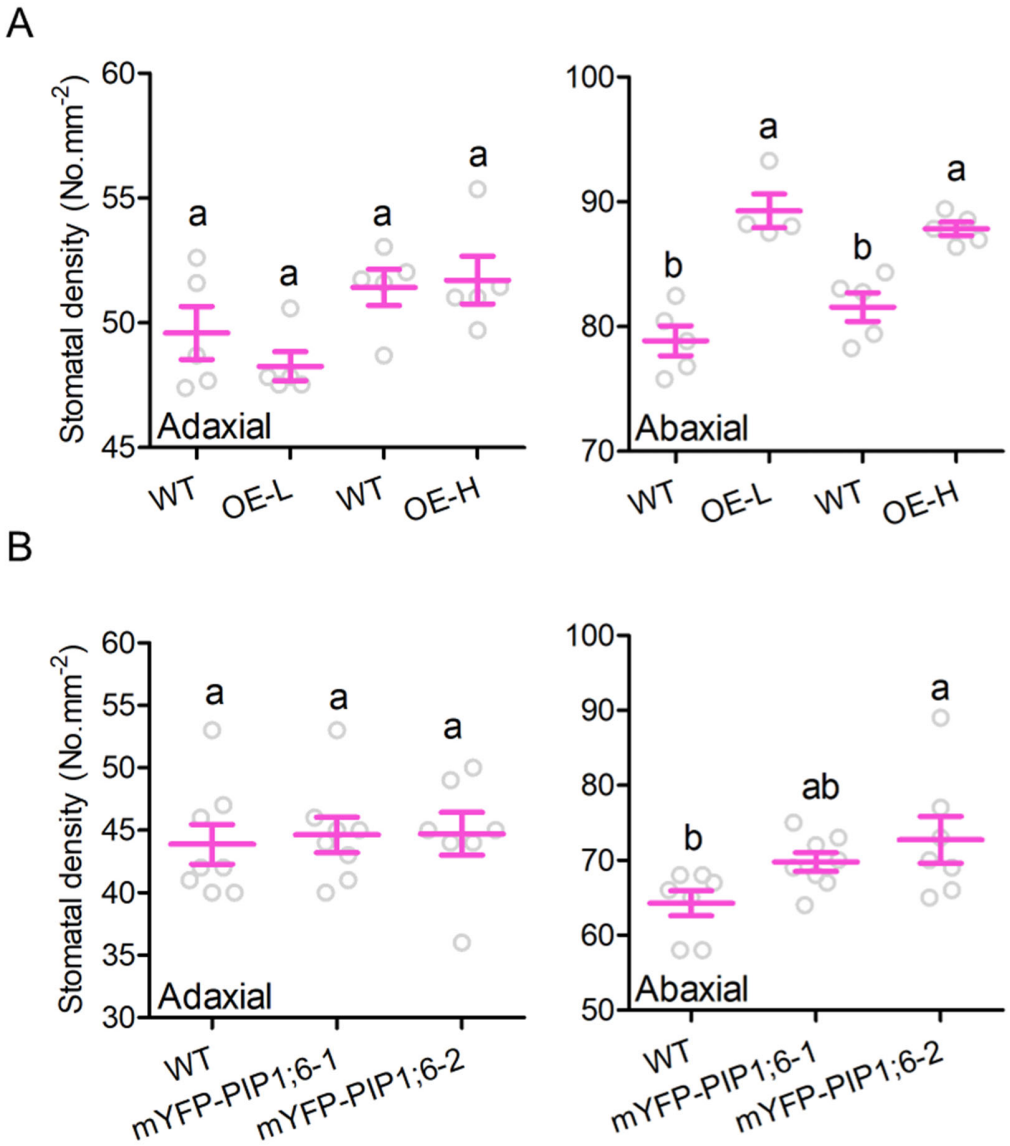

610

611

612 Figure 7

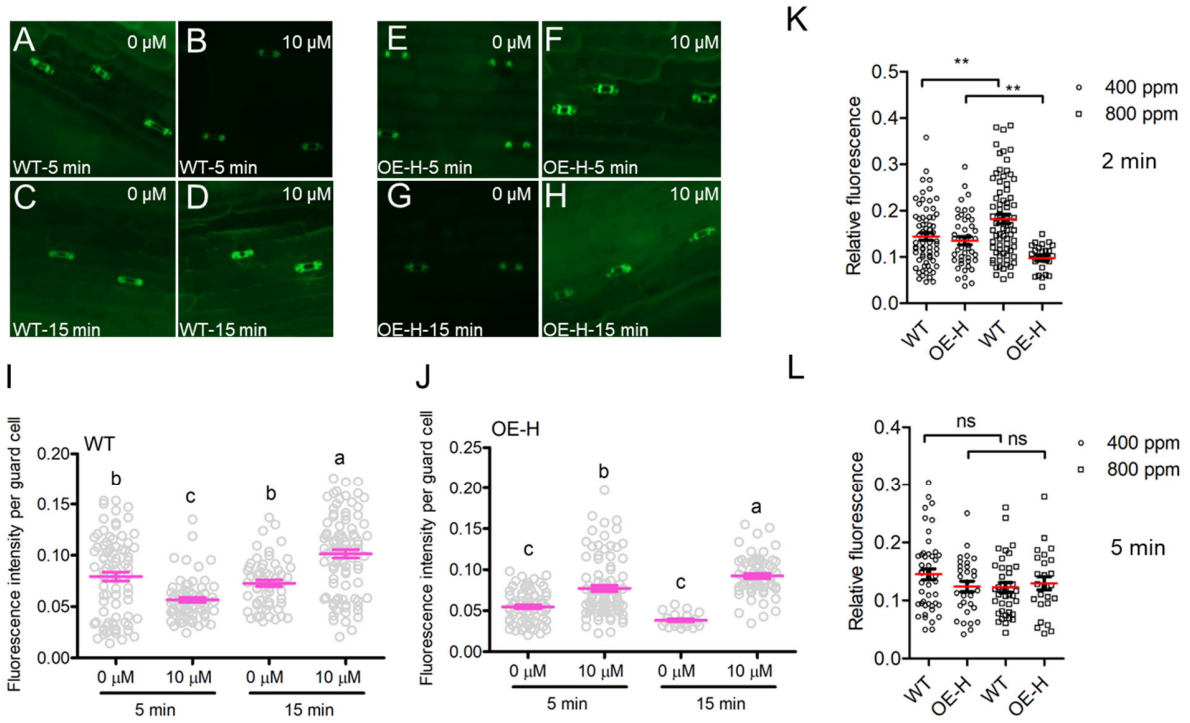

613

614

615 Figure 8

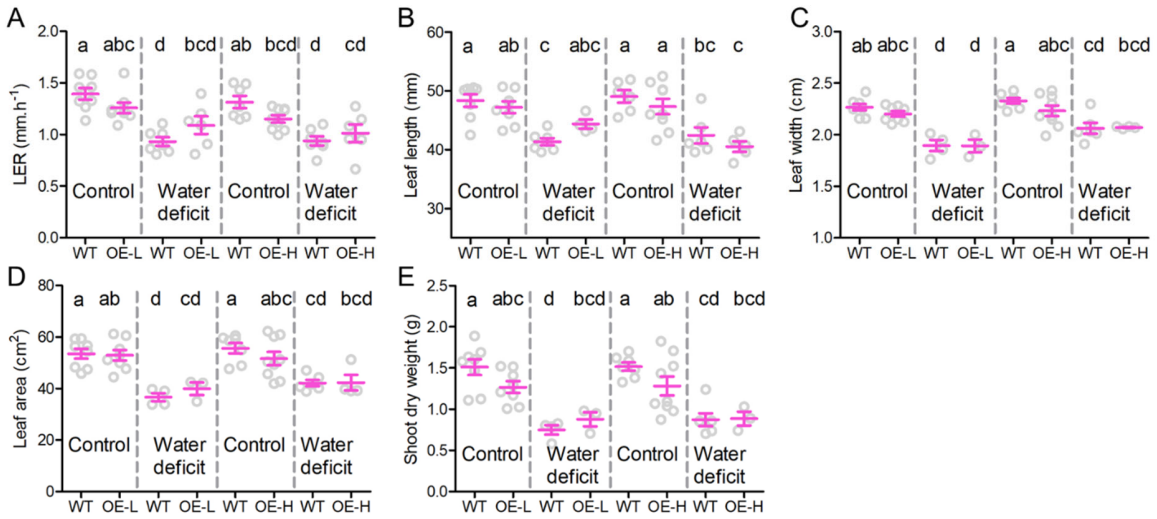

616

617

618 Table S1 List of primers used in this study

Genes	**Primers**
ZmPIP1;6 coding region	Forward: 5'GGTCTTAAUATGGCAGGAGGCACGCTG3' Reverse: 5'GGCATTAAUCTAGTAGTGAGCGCTGGAC3'
ZmPIP1;6 promoter (3449 bp)	Forward: 5`AGCTTTGGCTTCATCTATGT3` Reverse: 5`CTGCAGCGTGCCTCCTGCCAT3`
ZmPIP1;6 promoter (3000 bp)	Forward: 5`GGGGACAACTTTGTATAGAAAAGTTGAGCTTTGGCTTCATCTATGTTGTGG3` Reverse: 5`GGGGACTGCTTTTTTGTACAAACTTGGAATACTAACTCGCTCAGCTACGAT3`
mYFP-ZmPIP1;6	Forward: 5`GGGGACAAGTTTGTACAAAAAAGCAGGCTGTTAGTATTCATGGTGAGCAAGGGCGAG3` Reverse: 5`GGGGACCACTTTGTACAAGAAAGCTGGGTCTAGTAGTGAGCGCTGGACTTGAAG3`
Transgene insertion (p35S::ZmPIP1;6)	Forward: 5`CCACTATCCTTCGCAAGACCC3` Reverse: 5`GGTGATTTTTGCGGACTCTAGCAT3`
Transgene insertion	Forward: 5`ACGACGGCAACTACAAGACC3`

(pZmPIP1:6::mYFP-ZmPIP1;6)	Reverse: 5`CTCAGGTAGTGGTTGTCGGG3`
ef1α	Forward: 5'GATCTGAAGCGTGGGTATGTG3' Reverse: 5'GATGACCTGGGAGGTAAAGCTAG3'
actin1	Forward: 5'GCCCTGCTGTATGAAATGGA3' Reverse: 5'AAAGGAACCAGCTAAAAGCAAAC3'
Transgene PIP1;6	Forward: 5'TACCACCAGGTCGTCCTCAG3' Reverse: 5'ACGACGGCCAGTGAATTATC3'

619

620

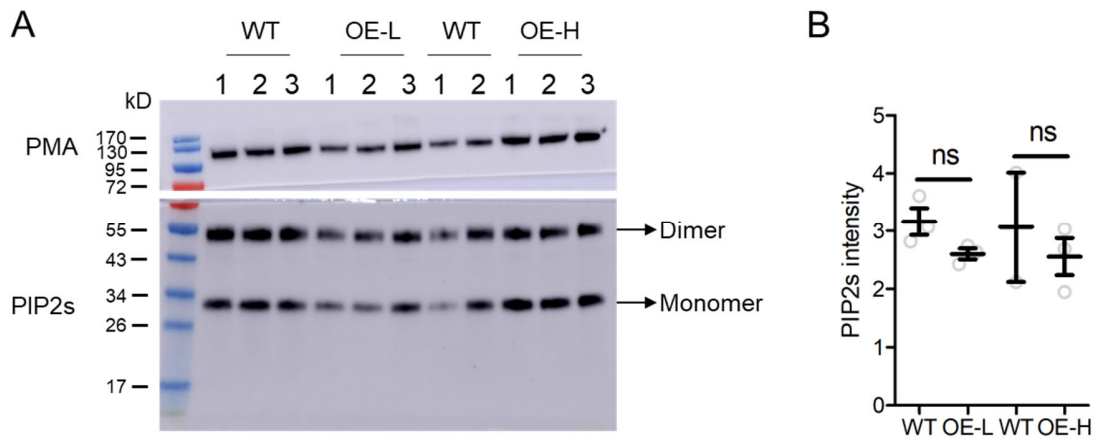

621

622 Fig. S1. ZmPIP2s protein expression in WT and ZmPIP1;6 OE plants. A, western blot signal.
623 Plasma membrane protein was extracted from whole leaves (leaves were pooled from n > 3
624 plants) and western blots were carried out using antibodies raised against ZmPIP2s and H^+-
625 ATPase (PMA, loading control). B, Western blot signal quantification. Data are expressed as the
626 mean ± SE. Student's *t* test was applied to compare the significant difference of PIP2s signal
627 between WT and OE plants. ns, not significant at level of $p < 0.05$. Plants were grown in
628 phytotron.

629

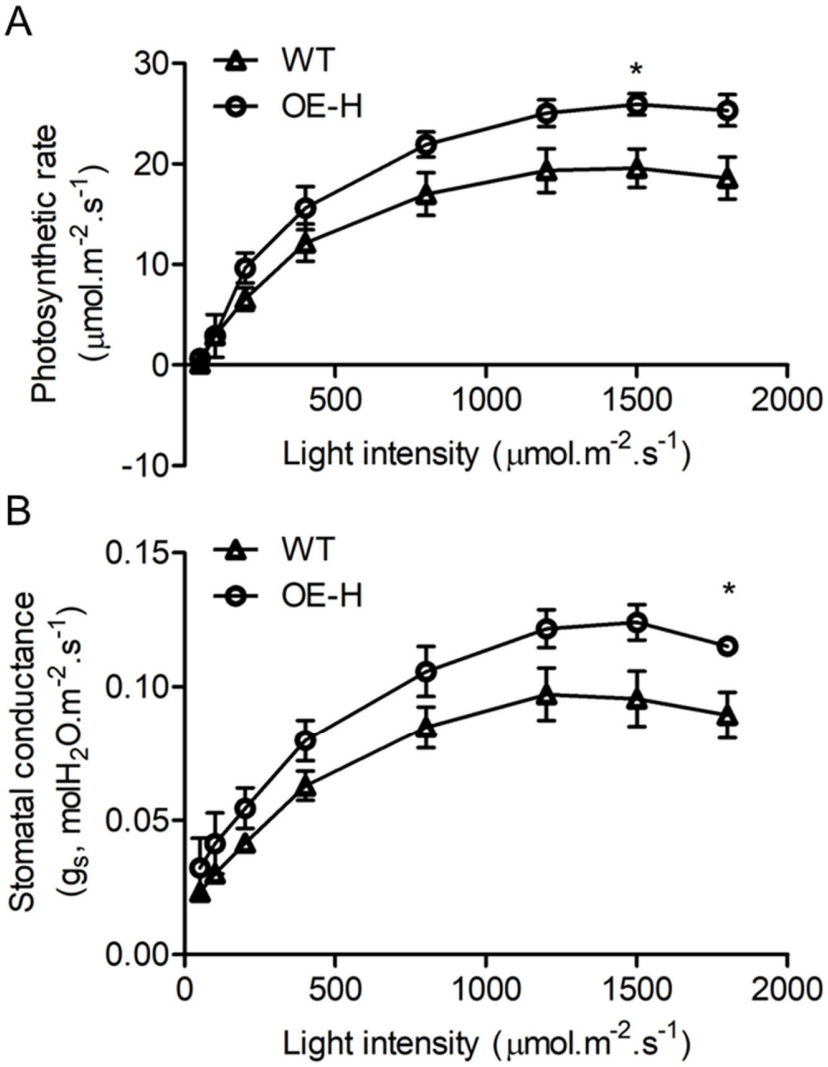

630

631 Fig. S2. Photosynthetic rate (A) and g_s (B) in responding to changing light intensity in WT and
632 OE-H plants. Data are expressed as the mean ± SE, n= 3 plants. Student's *t* test was applied to
633 compare the significant difference of A/g_s between WT and OE plants at the level of $*p<0.05$.
634 Plants were grown in greenhouse and the measurement was performed in greenhouse.

635

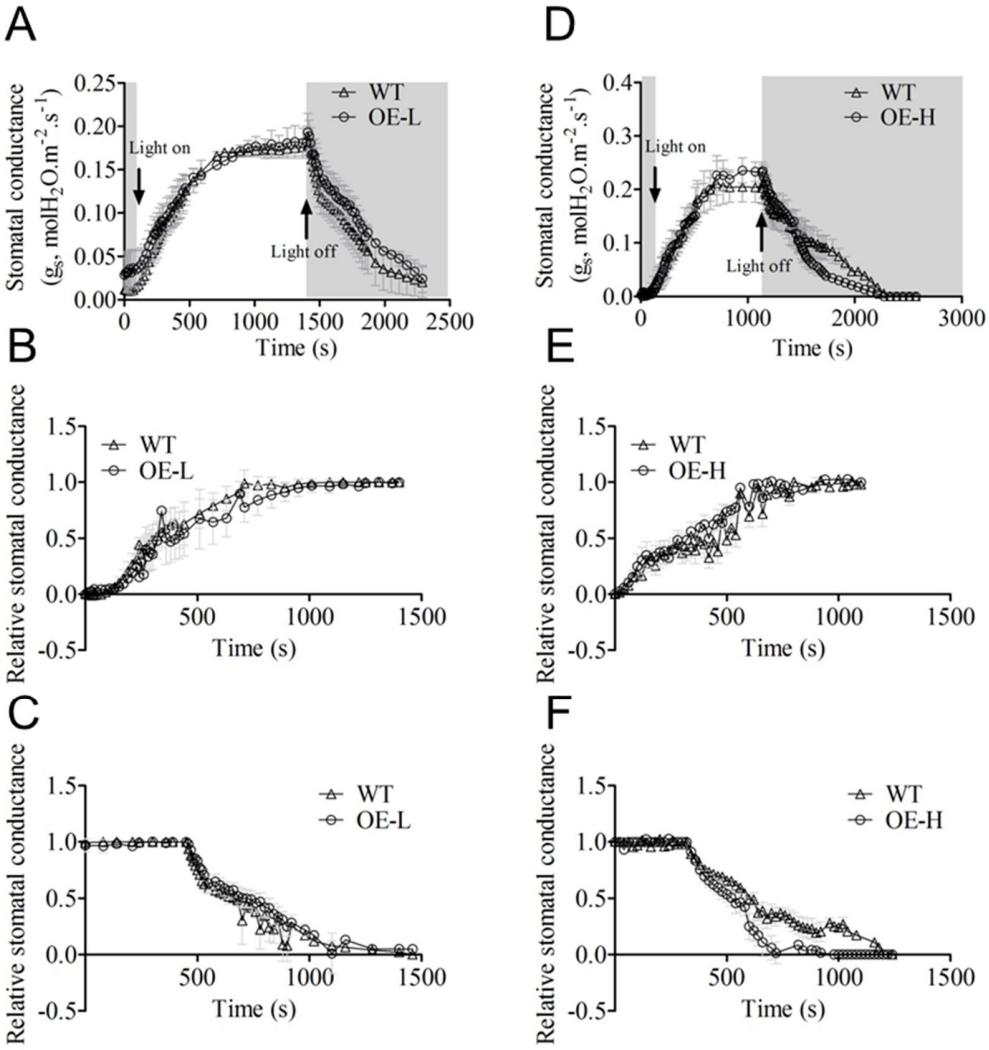

Fig. S3. The change of g_s in responding to light on and off in WT, OE-L (A-C) and OE-H (D-F) plants. A and D, continuously recording of g_s under light on/off treatments. B and E, relative increase of g_s under light on treatment. C and F, relative decrease of g_s under light off treatment. Data are expressed as the mean ± SE, n > 3 plants. Plants were grown in greenhouse and the measurement was performed in greenhouse.

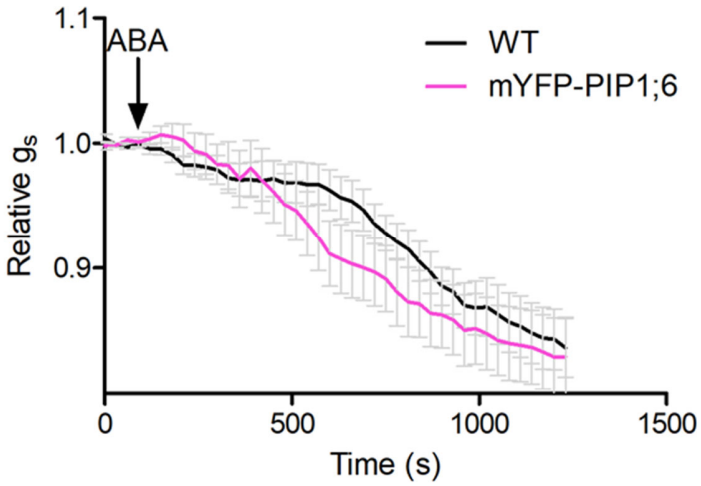

643

644 Fig. S4. Relative decrease of g_s in WT and mYFP-ZmPIP1;6 plants. Data are expressed as the
645 mean ± SE. Six WT and nine mYFP-ZmPIP1;6 leaves were measured. Plants were grown in
646 greenhouse and the measurement was performed in greenhouse.

647

648

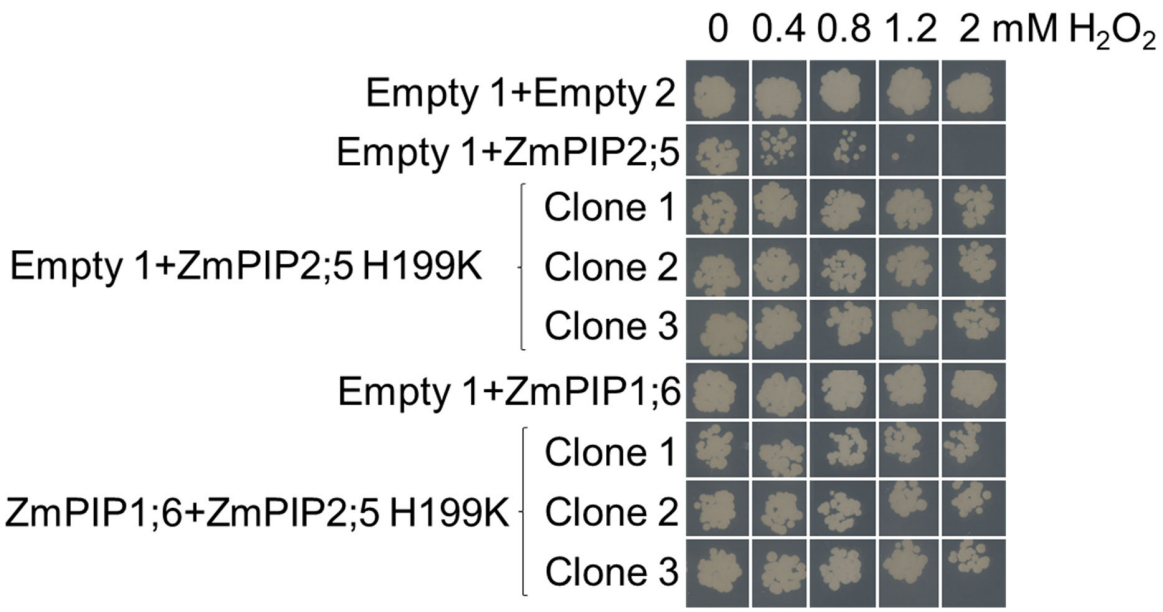

649

650 Fig. S5. H_2O_2 toxicity assay in yeast expressing ZmPIP1;6, ZmPIP2;5 and ZmPIP2;5 H199K
651 mutant. Empty 1, empty vector with leucine selection marker. Empty 2, empty vector with uracil
652 selection marker. ZmPIP2;5 H199K, ZmPIP2;5 mutant. When combination presenting, the cells
653 were co-transformed with two vectors with either leucine or uracil selection marker. Three
654 independent clones were selected for “Empty 1+ZmPIP2;5 H199K” and “ZmPIP1;6+ZmPIP2;5
655 H199K”. The indicated concentration of H2O2 was added to synthetic medium (2% (w/v)
656 galactose, 50 mM succinic acid/Tris base (pH = 6.5), 0.7% (w/v) YNB without amino acids, 0.3%
657 (w/v) methionine, 0.3% (w/v) histidine and 2% (w/v) agar), and an OD of 0.01 yeast culture was
658 dropped on the plate. Growth was assessed after 7 days at 30 ° C.

659